Biophysical Journal, Volume *110*

Supplemental Information

Chloride Anions Regulate Kinetics but Not Voltage-Sensor Q_{max} of the Solute Carrier SLC26a5

Joseph Santos-Sacchi and Lei Song

Supporting material

Removal of stray capacitance at C_m measuring frequencies

We use an Axon 200B patch clamp amplifier to measure OHC capacitance. Methodology was coded in jClamp and utilizes admittance measures at 2 frequencies to measure capacitance (1, 2). A linear cell model is depicted below, where Rs, Rm and Cm at each frequency (ω0, ω1) are derived from the following equations.

```
a0=real(Y) @ w0
a1=real(Y) @ w1
b0=imag(Y) @ w0
b1=imag(Y) @ w1

c0=a0^2 + b0^2;
c1=a1^2 + b1^2;

b=(-0.5) * (-c1+c0 + sqrt(c1^2 - 2*c1*c0 + c0^2 - 4*a1*a0*c1 + 4*a1^2*c0 + 4*a0^2*c1 -  4*a0*a1*c0)) / (a1-a0);

Rs0=(a0-b) ./ (a0.^2 + b0.^2 - a0*b);
Rm0=1/b * ((a0-b).^2 + b0.^2) ./ (a0.^2 + b0.^2 - a0*b);
Cm0=((1 ./ (w0.* b0)) .* ((a0.^2 + b0.^2 - a0*b).^2) ./ ((a0-b).^2 + b0.^2));

Rs1=(a1-b) ./ (a1.^2 + b1.^2 - a1*b);
Rm1=1/b * ((a1-b).^2 + b1.^2) ./ (a1.^2 + b1.^2 - a1*b);
Cm1=(1 ./ (w1.* b1)) .* ((a1.^2 + b1.^2 - a1*b).^2 ./ ((a1-b).^2 + b1.^2));
```

An example of our approach to remove stray capacitance is shown below using jClamp interfaced to a MatLab Simulink model. First, the model is evaluated without stray capacitance, where Rs= 10 Mohm, Rm=200 Mohm, Cm= 15 pF.

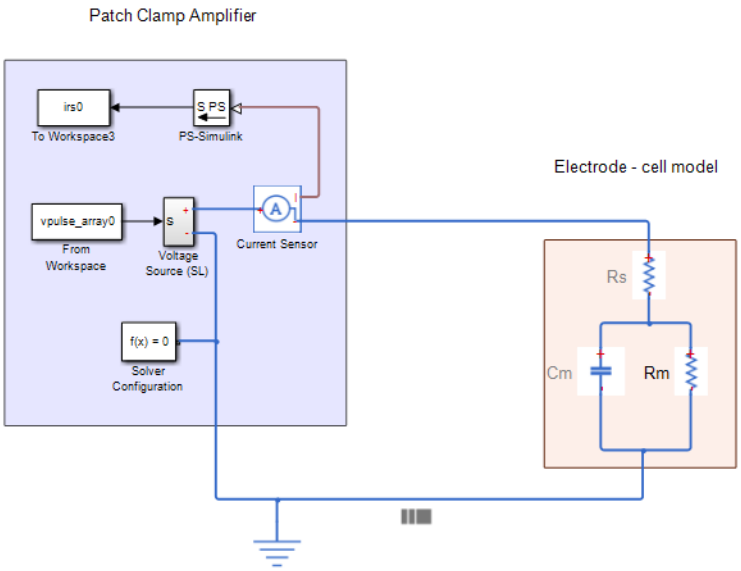

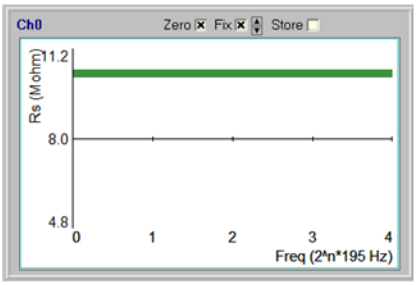

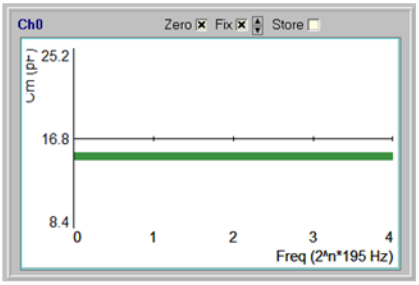

Note that the solutions (Rs and Cm plotted) provide exact parameter estimates regardless of frequency of stimulation (or, in fact, regardless of component values). However, real world recording includes parasitic capacitances, termed stray capacitance, the inclusion of which is modeled below.

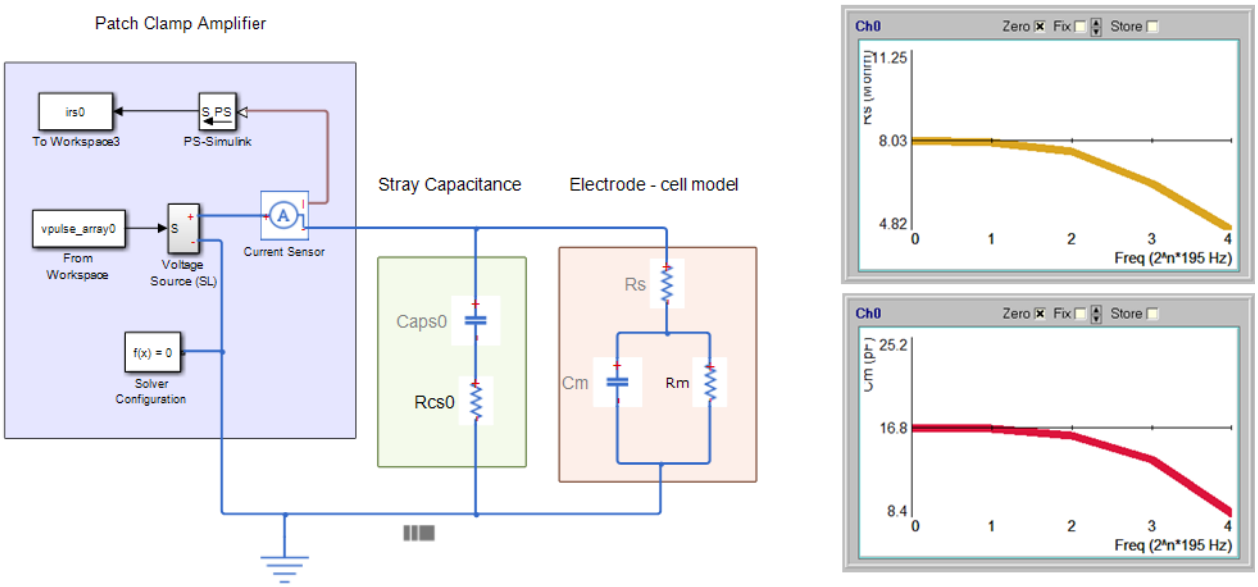

Here, utilization of the exact solutions above provides inaccurate measures, showing both Rs and Cm decreasing with increasing frequency. Both Rs and Cm are linear, and as defined are neither frequency nor voltage dependent. It behooves us then to remove stray capacitance effects during our recordings, since only without stray capacitance are our equations valid. Typically, stray capacitance effects (e.g., due to pipette holder and pipette – we use thick wall borosilicate glass pipettes coated with M-coat to reduce stray capacitance) are cancelled following gigohm seal formation during patch clamp recording by utilizing Axon 200B amplifier capacitance compensation controls. Unfortunately, this balancing procedure (using voltage steps in the time domain to cancel capacitive spikes) often is imperfect and stray capacitance effects can remain at our measurement frequencies. We attempt to overcome this problem after establishing whole cell configuration by stimulating in the frequency domain with a multi-frequency protocol that defines our interrogating frequencies. We then further fine balance with amplifier controls until calculated linear Cm and Rs are flat across frequency, as they should be. Any change in stray capacitance during the course of a recording session can be cancelled in this manner, e.g., if bath fluid levels changes. For our studies on synaptic activity (3-5), we can remove stray capacitance at any holding potential since the membranes of cells we study have no large intrinsic voltage dependent capacitance. However, in order to balance out stray capacitance for OHCs we hold the cell at positive potentials where linear capacitance dominates. Having succeeded in minimizing confounding effects of stray capacitance on linear membrane capacitance measurements across frequency, we then can investigate the frequency dependence of **NLC**. As detailed in the *Methods* section of our manuscript, Cm is measured at a range of holding potentials to generate a Cm-Vm plot that is fit with *eq. 1*, enabling extraction of Boltzmann characteristics, Qmax, Vh, and z. When sensor charge (Qmax) is plotted versus frequency of interrogation, we find that **NLC** is frequency dependent but linear capacitance is frequency independent (Fig. 2), confirming stray capacitance cancellation at our measuring frequencies. Our modelling indicates that the frequency dependence of **NLC** relates to the transition rates between conformational states of prestin.

Rs effects on membrane voltage drop and clamp time constant are removed with our methodology

Equipment frequency response (magnitude and phase of amplifier and associated equipment in the recording path) is corrected for by generating a calibration table across measurement frequencies, which is applied post-hoc to correct data for system response characteristics. This is a standard approach in all areas of system identification, including patch clamp assessment of Cm (6).

Our dual-sine analysis fundamentally corrects for effects of Rs, since it works by finding the parameter solutions of the total admittance of the patch clamp-cell circuit (as modelled above), given a known voltage across the total admittance. Thus, Cm derivation by this method takes into account the voltage drop across Rs at any frequency, providing true measures of Cm across frequency. Fits to Cm-Vm (or Q-Vm, in the case of current integrations) are made using corrected Vm values based on measured Rs, namely, Vm= Vcom – Irs * Rs, where the cell has been held sufficiently long to reach steady state voltage levels (in our case, for hundreds of ms before Cm analysis). Below, we show with electrical and mathematical models that Rs effects do not interfere with our Cm measures.

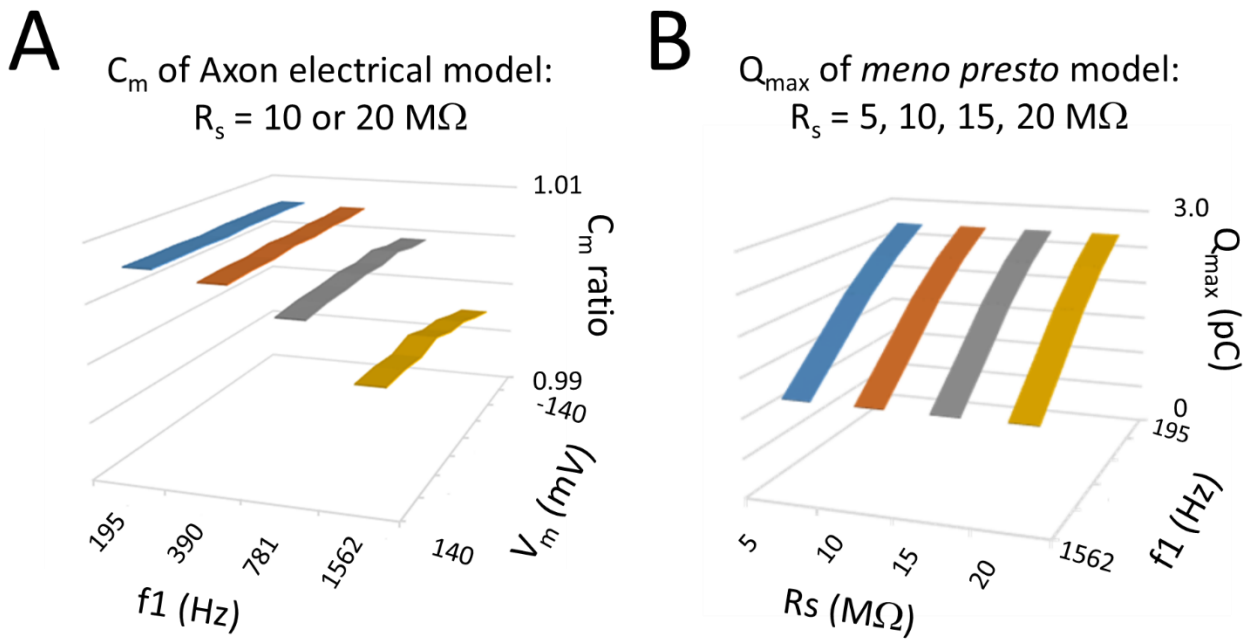

A) An electrical model cell was used to measure Cm, following stray capacitance cancellation as above. Model parameters were Rs=10 or 20MΩ, Rm = 500 MΩ, Cm= 33 pF. The plot shows that the ratios of Cm@20 MΩ/ Cm@10 MΩ measured at a range of holding potentials and frequencies (primary f1 frequency of dual-sine stimulus shown) are essentially identical (ratio ~ 1), regardless of Rs value. This indicates that Rs (with its influence on clamp time constant) does not affect our Cm frequency response measures in the absence of stray capacitance. Average Cm across voltages at 195 Hz was 33.0 pF for 10 MΩ Rs and 33.2 pF for 20 MΩ Rs. At 1562 Hz values were 33.1 pF for 10 MΩ Rs and 33.0 pF for 20 MΩ Rs. Differences arise form variability in stray capacitance cancellation, as is evident from model evaluations in B) in the absence of stray capacitance.

B) The *meno presto* model (7) was used to measure Cm-Vm functions that were fit to extract Qmax. Rs ranging from 5-20 MΩ has no effect on the magnitude *or* frequency response of NLC (Qmax), which is frequency-dependent due to model transition rates. Frequency is (plotted on a linear scale. Chloride set to 140 mM. Rm=200 MΩ, Clin=20 pF.

References

1. Santos-Sacchi, J. 2004. Determination of cell capacitance using the exact empirical solution of dY/dCm and its phase angle. Biophys J 87:714-727.
2. Santos-Sacchi, J., S. Kakehata, and S. Takahashi. 1998. Effects of membrane potential on the voltage dependence of motility-related charge in outer hair cells of the guinea-pig. J.Physiol 510 (Pt 1):225-235.
3. Ricci, A. J., J.-P. Bai, L. Song, C. Lv, D. Zenisek, and J. Santos-Sacchi. 2013. Patch-Clamp Recordings from Lateral Line Neuromast Hair Cells of the Living Zebrafish. Journal of Neuroscience 33:3131-3134.
4. Schnee, M. E., J. Santos-Sacchi, M. Castellano-Munoz, J. H. Kong, and A. J. Ricci. 2011. Calcium-dependent synaptic vesicle trafficking underlies indefatigable release at the hair cell afferent fiber synapse. Neuron 70:326-338.
5. Schnee, M. E., J. Santos-Sacchi, M. Castellano-Munoz, J. H. Kong, and A. J. Ricci. 2011. Tracking vesicle fusion from hair cell ribbon synapses using a high frequency, dual sine wave stimulus paradigm. Communicative & Integrative Biology 4:785-787.
6. Gillis, K. D. 1995. Techniques for Membrane Capacitance Measurements. In Single Channel Recording. B. Sakmann, and E. Neher, editors. Plenum Press, New York. 155-198.
7. Santos-Sacchi, J., and L. Song. 2014. Chloride and Salicylate Influence Prestin-dependent Specific Membrane Capacitance. Journal of Biological Chemistry 289:10823-10830.